Int J Earth Sci (Geol Rundsch) (2013) 102:1091–1109
DOI 10.1007/s00531-012-0850-8

ORIGINAL PAPER

Phase equilibrium, geothermobarometric and xenotime age dating constraints on the Alpine metamorphism recorded in chloritoid schists from the southern part of the Tisia Mega-Unit (Slavonian Mts., NE Croatia)

Dražen Balen · Péter Horváth · Fritz Finger · Biljana Starijaš

Received: 20 May 2012 / Accepted: 25 November 2012 / Published online: 14 December 2012

Abstract The chloritoid schists from the Slavonian Mts., which are attributed to the basal part of Devonian to Permian "Hercynian Semimetamorphic Complex," represent a very rare lithology, not only in the Tisia Mega-Unit outcrops in Croatia, but also in the wider area. The investigated outcrop in the Kutjevačka Rijeka transect (Mt. Papuk) encompasses chloritoid-bearing metapelitic and metapsammitic lithologies. Both contain K-white mica, chlorite, chloritoid (10–15 vol.%), quartz and minor K-feldspar, plagioclase (albite), opaque minerals and pyrophyllite, together with accessory zircon, rutile, xenotime. The Th–U–Pb age dating on xenotime grains within the K-white mica + chlorite + quartz matrix and on inclusions found inside the chloritoids gave an average age 120 ± 36 Ma. Peak metamorphic conditions during the Alpine chloritoid-forming event reached 3.5–4 kbar and 340–380 °C, based on phengite barometry, chlorite–chloritoid thermometry and intersection of chlorite and chloritoid isopleths in the KFMASH quantitative phase diagram. The post-tectonic character of lath- and rosette-shaped chloritoids with respect to two foliations in the rock, together with the older age of 219 ± 81 Ma obtained on Yb-rich xenotime core domain(s), implies a possible existence of older low-grade metamorphic phase(s). The chemistry of the chloritoid schists bears the signature of upper continental crustal felsic rocks as potential protoliths, probably the felsic rocks of the nearby Papuk Complex of Slavonian Mts. The evidence presented here for the chloritoid-bearing low-grade metamorphic rocks from the Slavonian Mountains clearly show that the prograde Alpine metamorphic event had a more significant influence on the evolution of the southern part of Tisia Mega-Unit than previously considered.

Keywords Chloritoid schist · Xenotime · Low-grade metamorphism · Alpine imprint · Slavonian Mts. · Tisia

D. Balen (✉)
Department of Geology, Faculty of Science,
University of Zagreb, Horvatovac 95,
10000 Zagreb, Croatia
e-mail: drbalen@geol.pmf.hr

P. Horváth
Institute for Geochemical Research, Hungarian Academy of Sciences, Budapest, Hungary

Present Address:
P. Horváth
MOL Plc Exploration and Production Division,
Reservoir and Technology Engineering, Budafoki str 79.,
Budapest 1117, Hungary

F. Finger · B. Starijaš
Division of Mineralogy, Department of Materials Engineering and Physics, University of Salzburg, Hellbrunnerstrasse 34,
5020 Salzburg, Austria

Introduction

Metapelites are, in the general sense, rocks that are very sensitive to changes of metamorphic conditions and can be excellent tracers for *P–T* estimation of metamorphic event(s). However, in the field of low-grade metamorphism, recognition of chemical and structural equilibrium may not be straightforward and the lack of suitable low-variance assemblages can present a severe problem. One among very few minerals applicable to quantitative definition of low-grade metamorphism is chloritoid as a characteristic mineral in low-temperature Al-rich metapelitic rocks. Its ability to change chemical composition in respect to the changes of metamorphic conditions makes it an

appropriate phase for recording *P–T* conditions in low-grade metamorphic rocks. Fe-rich chloritoid is characteristically found in low-grade metamorphic rocks, whereas the Mg-rich chloritoid is a typical mineral of high-pressure metamorphism (e.g., Chopin 1983; Chopin and Monié 1984; Simon et al. 1997; Messiga et al. 1999). Consequently, both chloritoid varieties are important phases for geothermometric and geobarometric purposes. The stability field of Fe-chloritoid has been defined by Vidal et al. (1994), whereas Chopin (1985) examined the stability of Mg-chloritoid.

The term "Hercynian Semimetamorphic Complex" (HSC) of Slavonian Mountains was introduced by Jamičić and Crnko describing the Unit no. 8 in the most recent geological map of Croatia and accompanying explanatory note (Velić and Vlahović 2009). HSC consists of different types of very low to low-grade metamorphic rocks and unmetamorphosed rocks, representing an important lithological association but mostly without any key mineral for extracting reliable quantitative thermobarometric data. This complex typically comprises graphite-bearing metagreywackes in its lower part, which show unconformable contact to Lower Paleozoic low- to medium-grade metamorphic rocks. Locally, in that lower part of complex, pelitic schists with chloritoid, chlorite, white mica and quartz as major phases in the mineral assemblage can be found. Since occurrences of chloritoid schists are extremely rare, not only in the Slavonian Mountains but also in the other basement outcrops of Pannonian Basin area (for list see Vragović and Majer 1979a, b; Koroknai et al. 2000, 2001; Belak 2005), its potential to preserve information about *P–T* conditions and the age of origin gives it an important role in solving the origin of HSC low-grade schists. Also, it could be a marker lithology in explaining the complexity of geological evolution (Variscan and Alpine) of the Slavonian Mountains and the Tisia Mega-Unit.

The aim of the paper is to clarify the nature and origin of the chloritoid schists using a multidisciplinary approach, particular attention being paid to the extraction of *P–T* data and the age of the metamorphism.

Geological setting

From the regional point of view, crystalline rocks of the Slavonian Mountains, located in NE Croatia on the SW edge of Pannonian Basin toward the Dinarides, belong to the Tisia Mega-Unit. This large tectonic unit (Fig. 1a inset), which is the southeastern megatectonic unit of the Pannonian Basin basement, is commonly regarded as a lithospheric fragment broken off from the southern margin of the European plate by the Middle Jurassic opening of the eastern branch of the Alpine Tethys (Géczy 1973; Csontos 1995; Pamić et al. 2002; Schmid et al. 2008 and references therein). The Tisia Mega-Unit reached its present-day position after complex regional-scale translational and rotational movements during the Mesozoic and Cenozoic (Csontos 1995; Fodor et al. 1999; Csontos and Vörös 2004). These motions were controlled by the major tectonic contact zones of the Alpine–Carpathian–Dinaridic orogenic system, most of them representing oceanic sutures (Schmid et al. 2008). According to regional reconstruction after Schmid et al. (2008), the internal structure of Tisia Mega-Unit encompasses three huge southward dipping Alpine nappe systems called Mecsek, Bihor and Codru, each comprising crystalline basement rocks and post-Variscan overstep sequences. From the point of view of such large-scale reconstruction, Slavonian Mountains belong to the Bihor nappe system.

The Slavonian Mts. comprise four hills, reaching up to 1,000 m height: Psunj, Ravna Gora, Papuk and Krndija (Fig. 1a). These hills together form the largest single exposure of pre-Alpine crystalline basement in the southern part of the Tisia Mega-Unit (e.g., Pamić and Jurković 2002; Pamić et al. 2002). The crystalline basement is locally covered by Upper Permian to Mesozoic sediments and the Neogene–Quaternary fill of the Pannonian Basin (Jamičić 1989; Jamičić and Brkić 1987). The pre-Alpine crystalline basement of Slavonian Mountains is further subdivided by Jamičić (1983, 1988) into three complexes (Fig. 1): (1) greenschist to medium-grade Psunj (Kutjevo) Complex (PsC) comprises mostly greenschists, micaschists, gneisses, amphibolites, metagabbros and I-type granitoids; (2) Papuk (Jankovac) Complex (PaC), which underwent medium- to high-grade metamorphism and migmatization, comprises migmatites, gneisses, micaschists and S-type granites, and (3) very low-grade Radlovac Complex (RaC). The RaC, also called "Semimetamorphic Complex with Metadiabases" (Pamić and Lanphere 1991), consists of the (very) low-grade (sub-greenschist facies) metamorphic sequences largely composed of slates, metagraywackes, metaconglomerates with subordinate phyllites, locally intruded by metabasic rocks (Pamić and Jamičić 1986). It is unconformably covered by the clastic–carbonate succession of Upper Permian and Triassic age. Recently, monazite age dating showed complex metamorphic history of PsC with Ordovician–Silurian (444 ± 19 and 428 ± 25 Ma; Balen et al. 2006) and Variscan (356 ± 23 Ma; Horváth et al. 2010) ages. The K–Ar ages for PaC show Late Paleozoic ages (336–324 Ma; Pamić et al. 1988), while for the RaC Cretaceous K–Ar ages have been reported (Biševac et al. 2010).

According to the Basic geological map—sheet Orahovica (Jamičić et al. 1986; Jamičić and Brkić 1987), chloritoid schists mark a narrow zone in the Kutjevačka

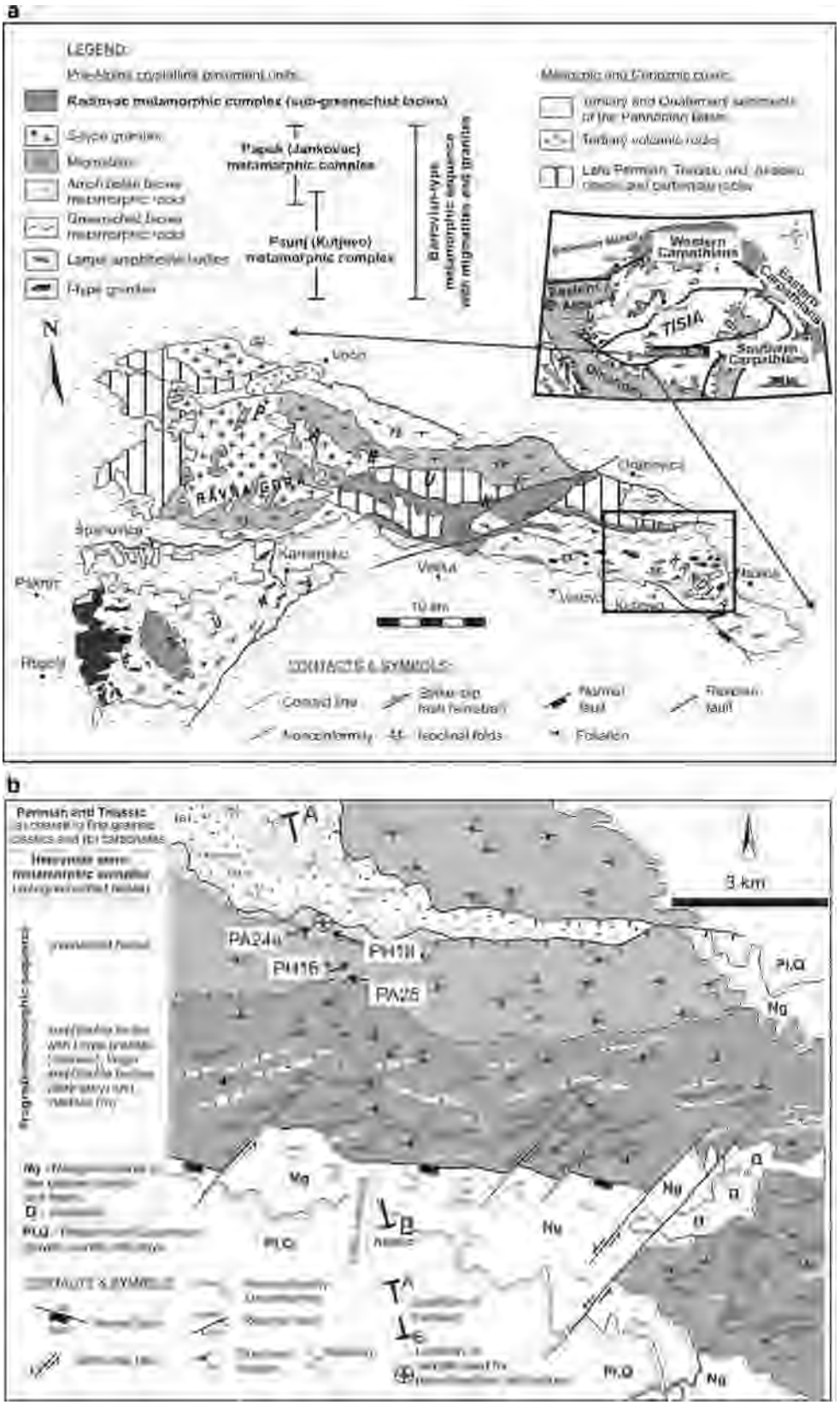

Fig. 1 **a** Simplified geological map of the Slavonian Mts. (after Jamičić and Brkić 1987; Jamičić 1988; Pamić and Lanphere 1991) with index map showing the position of the Tisia Mega-Unit within the Pannonian Basin. *Box* shows the relative position of the studied area enlarged on Fig. 1b. **b** Geological setting of the studied area with the location of the investigated outcrops and trace of Kutjevačka Rijeka transect (*A*–*B*). Maps are taken from Balen et al. (2006) and Horváth et al. (2010) and were slightly modified

Rijeka transect area (Fig. 1), presumably of Upper Devonian age, separating the older metamorphic complex (PsC) from the Permo-Triassic sedimentary rocks. Recent view of Jamičić and Crnko in Velić and Vlahović (2009) is that graphite-bearing metagraywackes and chloritoid schists are basal part of Devonian to Permian HSC which unconformably overlies the older Paleozoic rocks. The paleontological age of metagraywacke and metasandstone protoliths, which were continuously deposited onto the basal graphite-bearing metagraywackes and chloritoid schists, is Late Carboniferous (Westphalian B and C) based on microflora findings (Brkić et al. 1974). The thickness of (meta) sedimentary column, from the part comprising chloritoid schists up to the Westphalian rocks, is approx. 1,000 m (according to Fig. 7 in Jamičić 1988).

Materials and methods

Whole-rock chemistry

From the selection of dozen hand-specimens, four rock samples including various types of chloritoid schists and PsC chlorite schists were analyzed in ACME Analytical Laboratories Ltd., Vancouver (Canada) by the ICP-MS (trace elements including REE) and ICP-ES (major elements) following a sample fusion. The air-dried samples were sieved to pass 0.125 mm stainless-steel screen and were analyzed for the following elements: Si, Ti, Al, Fe, Mn, Mg, Ca, Na, K, P, Cr, Ba, Co, Cs, Cu, Ga, Hf, Nb, Ni, Pb, Rb, Sc, Sr, Ta, Th, U, V, Y, Zn, Zr, La, Ce, Pr, Nd, Sm, Eu, Gd, Tb, Dy, Ho, Er, Tm, Yb and Lu. Sample preparation included splitting of 0.2 g sample for $LiBO_2$/$Li_2B_4O_7$ fusion decomposition for ICP-ES and 0.2 g sample for ICP-MS. Analysis by ICP-MS used the method of internal standardization to correct for matrix and drift effects. Natural rocks of known composition and pure quartz were used as reference standards. The analytical accuracy was controlled using the internal geological reference materials DS8, OREAS45CA, SO-18, GS311-1 and GS910-4 which represent comparable materials. The reference materials were certified in-house by analysis with CANMET Certified Reference Materials. Loss on ignition (LOI) is determined by weight difference after 4-h ignition at 1,000 °C.

Mineral chemistry

Electron microprobe analyses were performed on selected rock samples at the Institute for Geochemical Research, Hungarian Academy of Sciences using a JEOL JCXA-733 electron microprobe equipped with an Oxford INCA 200 EDS. Operating conditions were 20 keV accelerating voltage, 4 nA sample current and 100 s counting time. The PAP correction procedure was applied (Pouchou and Pichoir 1984). The following standards were used: albite for Na, quartz for Si, corundum for Al, periclase for Mg, orthoclase for K, apatite for Ca, hematite for Fe, spessartine for Mn and rutile for Ti.

BSE imaging and microprobe analyses of xenotime were performed on a JEOL JXA-860 at Salzburg University. The analyses were carried out in wavelength dispersive mode. Element lines were chosen according to the recommendations of Pyle et al. (2002). Pb was determined on the Mβ line, and an exponential background correction was applied, following a careful inspection of the background patterns of different xenotime domains (Hetherington et al. 2008). Apart from Th, U, Pb, the elements P, Y, Si, Nd, Sm, Gd, Dy, Er and Yb were analyzed. Commercially available calibration standards were used (regarding the standard set and other analytical details see Krenn et al. 2008). In order to attain a reasonably precise analysis of the Pb in the range of ±0.005 wt% (2σ), the probe current was set to 250 nA at 15 kV, and long counting times of 400–800 s were used for peak and background acquisition. Counting times for the Th and U were 30 and 50 s, respectively. All other elements were determined with 10 s counting time intervals.

P–T pseudosections and geothermobarometry

Pseudosection modeling was undertaken with the 3.33 version of the THERMOCALC software (Powell et al. 1998) with the internally consistent thermodynamic dataset 5.5 (Holland and Powell 1998; January 2008 upgrade). The datafile coding of the activity–composition relationships of the minerals used in the KFMASH pseudosection calculations is that of Holland and Powell (1998) and Holland et al. (1998).

Besides pseudosection modeling, additional independent geothermometric calculations on the chloritoid-bearing assemblages were made using chlorite–chloritoid geothermometry after Vidal et al. (1999) while minimum pressure was defined after Massonne and Schreyer (1987) calibration based on the phengite content of white mica and extensions of calibration by Coggon and Holland (2002) and Caddick and Thompson (2008).

Results

The chloritoid schists were found in a narrow zone outcropping in the upper portion of the Kutjevačka Rijeka transect (Balen et al. 2006; Horváth et al. 2010) in the eastern Mt. Papuk area (Fig. 1b). Outcrop-scale and microstructural observations reveal two generations of

foliation in these rocks: 1. the older, closely spaced foliation (S_1) defined by parallel orientation of white mica and chlorite and 2. the younger one (S_2), crenulating the older foliation. The second foliation cuts the first one at high angle resulting in a characteristic wedge-shaped splitting of the rocks. Growth of chloritoids postdates foliations and a major folding event (Fig. 2).

Petrography

The samples are usually fine-grained phyllites with small dark spots belonging to chloritoid porphyroblasts. The rocks, variably colored (green, reddish, gray, black), show silky luster on the surface together with well-developed foliation and crenulation cleavage. The silky luster appearance is due to high modal content of white mica. The rock is composed of fine-grained K-white mica (illite–muscovite) up to 60 vol.%, chlorite, chloritoid, quartz, and minor K-feldspar, plagioclase (albite), opaque minerals (hematite, magnetite?), pyrophyllite and accessory phases: zircon, rutile, xenotime. The 0.2–0.5 mm large, dark chloritoid grains occupy up to 10–15 vol.% of the rock. They occur as randomly oriented single idioblastic, lath-shaped porphyroblasts or in the form of rosettes (clusters of sub-radiating grains) overgrowing the S_2 foliation (Fig. 2a, b). The grains show polysynthetic twinning and weak pleochroism (pale yellow to green; gray bluish). Among predominantly fine-grained samples, medium-grained, less homogeneous samples also occur, containing coarser grains of quartz which classify such samples as metasandstones. In that type of samples, chloritoid has grown in the fine-grained matrix areas between quartz grains.

Whole-rock chemistry

Samples of chloritoid schists (metapelitic PA24a and metapsammitic PH18 specimen), together with the chlorite schist (representing underlying PsC rocks) from the Kutjevačka Rijeka transect and representative granitoid rocks from PaC (metagranite) and PsC (granitoide), were analyzed for major, minor and trace elements (Table 1). The bulk composition of chloritoid schists corresponds well to an Al-rich pelitic composition, and they show higher Al_2O_3 (19.86–22.97 vs. 14.51–17.75 wt%), Fe_2O_3 (7.22–8.69 vs. 5.47–6.16 wt%) and lower SiO_2 (58.3–60.9 vs. 63.3–69.5 wt%), Na_2O (0.24–0.33 vs. 1.76–2.24 wt%) and CaO (0.02–0.07 vs. 0.66–0.89 wt%) contents compared to the PsC chlorite schists to which they show unconformable contact. The chloritoid schists show an increase in Rb (143–199 vs. 66–108 ppm), Ba (845–862 vs. 392–608 ppm), U (5–8 vs 1–2 ppm), Th (16–17 vs. 5–7 ppm), REEs, HFSE (Zr, Hf, Nb Y), Sc (19–20 vs. 11–14) and depletion in Sr and P (as highly soluble mobile ions) compared to the PsC chlorite schists. As expected for metamorphic rocks of sedimentary origin, the upper crust, North American Shale Composite (NASC) and European Shale (ES) normalized REE patterns are flat for both, chloritoid and chlorite schists. The chloritoid schists are REE enriched in comparison with NASC composition and also relative to the PsC chlorite schists samples. Total REE values range between 187 and 197 ppm for chloritoid schists, which is considerably higher than for the chlorite schists (90–114 ppm). Values for Cr, V, Ni in chloritoid schists are not significantly different from the values for the Upper Continental Crust (UCC). UCC-normalized (Taylor and McLennan 1985) trace element composition and chondrite-normalized (Boynton 1984) rare earth element (REE) patterns of the Kutjevačka Rijeka transect chloritoid schists and PsC chlorite schists show significant differences (Fig. 3a, b). The PaC metagranite shows pattern similar to the chloritoid schists, while PsC granitoid pattern resembles chlorite schists, both felsic rocks given as a reference (Fig. 3b).

The immobile elements likely reflect the composition of the sedimentary protoliths of the chloritoid schists. These protoliths are dominantly derived from felsic/granitoid

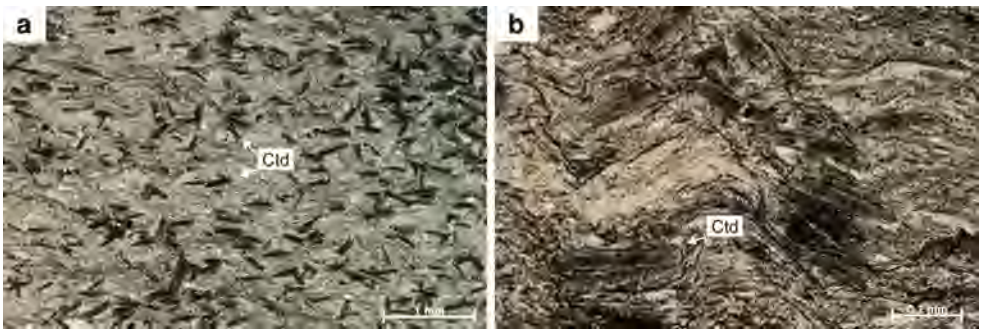

Fig. 2 Microfabric of chloritoid schist from Kutjevačka Rijeka transect showing. **a** Post-tectonic lath-shaped chloritoid grains and chloritoid rosettes in a fine-grained matrix of chlorite, white mica and quartz. **b** Crenulation cleavage in the chloritoid schist with post-tectonic growth of chloritoid. *Ctd* chloritoid

Table 1 Selected whole-rock analyses and characteristic elemental ratios and parameters for chloritoid schists, chlorite schists, representative felsic rocks for Psunj (PsC) and Papuk (PaC) Complex and upper continental crust as reference value

	ctd schists		chl schists PsC		I-granitoid	Metagranite	UCC	d.l. (wt%)
Sample	PA24a	PH18	PH16	PA25	PsC PA 28	PaC 105	McLennan (2001)	
Major elements (wt%)								
SiO_2	58.27	60.93	63.26	69.52	56.12	74.46	66.00	0.01
TiO_2	0.94	0.81	0.83	0.64	1.02	0.34	0.68	0.01
Al_2O_3	22.97	19.86	17.75	14.51	20.17	12.39	15.20	0.01
Fe_2O_3	7.22	8.69	6.16	5.47	6.08	2.59	5.03	0.04
MnO	0.10	0.09	0.11	0.10	0.10	0.02	0.08	0.01
MgO	2.03	2.19	2.24	2.10	2.16	0.72	2.20	0.01
CaO	0.02	0.07	0.89	0.66	5.79	0.66	4.20	0.01
Na_2O	0.33	0.24	1.76	2.24	4.87	3.71	3.90	0.01
K_2O	3.59	2.73	3.14	1.97	1.12	3.39	3.40	0.01
P_2O_5	0.03	0.09	0.08	0.08	0.28	0.07	0.15	0.01
LOI	4.30	4.10	3.60	2.60	2.10	1.50		0.01
Total	99.80	99.80	99.82	99.89	99.80	99.88		
Trace elements (ppm)								
Ba	862	845	608	392	331	227	550	1
Co	18.7	15.0	20.3	17.3	8.2	1.6	17	0.2
Cr	96	89	75	62	21	21	83	14
Cs	9.5	6.0	4.6	2.9	0.7	1	5	0.1
Cu	6.2	2.2	15.4	9.4	10.4	0.6	25	0.1
Ga	28.4	24.0	20.4	14.8	20.5	15.8	17	0.5
Hf	4.5	4.2	3.8	3.8	6.5	6.4	5.8	0.1
Nb	17.4	15.3	13.0	10.3	4.2	9.7	12	0.1
Ni	36.1	42.3	39.7	31.3	2.7	2	44	0.1
Pb	2.7	2.7	3.0	3.0	9.6	1.9	17	0.1
Rb	198.5	143.2	108.2	65.6	35	117.1	112	0.1
Sc	20	19	14	11	11	8	13.6	1
Sr	93.8	69.7	151.8	123.9	664.3	47.8	350	0.5
Ta	1.4	1.4	0.8	0.7	0.3	0.7		0.1
Th	16.4	16.9	7.2	5.4	1.7	25.4	10.7	0.2
U	8.2	5.4	1.5	1.1	0.7	1.9	2.8	0.1
V	125	104	102	72	91	45	107	2
Y	31.2	25.6	17.1	13.4	19.6	43.1	22	0.1
Zn	46	61	87	82	59	15	71	1
Zr	156.6	145.6	145.3	134.4	270.9	186.4	190	0.1
La	38.6	42.7	22.0	18.9	13.9	45.3	30	0.1
Ce	77.1	82.1	49.9	37.1	26.4	98.3	64	0.1
Pr	8.93	9.4	5.27	4.48	4.01	11.08	7.1	0.02
Nd	33.4	35.7	20.0	16.7	17	40.7	26	0.3
Sm	6.35	6.87	3.85	3.18	3.93	8.12	4.5	0.05
Eu	1.36	1.29	0.87	0.74	1.34	0.51	0.88	0.02
Gd	5.74	5.59	3.41	2.6	3.99	7.51	3.8	0.05
Tb	1.04	0.85	0.56	0.44	0.67	1.31	0.64	0.01
Dy	5.74	4.96	3.15	2.39	3.66	7.49	3.5	0.05
Ho	1.15	1.00	0.62	0.49	0.74	1.51	0.8	0.02
Er	3.43	3.11	1.93	1.54	2.08	4.18	2.3	0.03
Tm	0.51	0.46	0.32	0.24	0.31	0.6	0.33	0.01

Table 1 continued

	ctd schists		chl schists PsC		I-granitoid	Metagranite	UCC	d.l. (wt%)
Sample	PA24a	PH18	PH16	PA25	PsCPA 28	PaC105	McLennan (2001)	
Yb	3.61	2.86	2.21	1.59	2.11	3.34	2.2	0.05
Lu	0.44	0.45	0.33	0.26	0.32	0.52	0.32	0.01
SiO_2/Al_2O_3	2.54	3.07	3.56	4.79	2.78	6.01	4.34	
K_2O/Na_2O	10.88	11.38	1.78	0.88	0.23	0.91	0.87	
Na_2O/K_2O	0.09	0.09	0.56	1.14	4.35	1.09	1.15	
K/Cs	3137	3777	5667	5639	13282	28142	6136	
Zr/Hf	35	35	38	35	42	29	32.8	
Zr/Sc	8	8	10	12	25	23	14	
Zr/Th	10	9	20	25	159	7	18	
Th/Co	0.9	1.1	0.4	0.3	0.2	15.9	0.6	
Th/Cr	0.2	0.2	0.1	0.1	0.1	1.2	0.1	
Th/Sc	0.8	0.9	0.5	0.5	0.2	3.2	0.8	
Th/U	2.0	3.1	4.8	4.9	2.4	13.4	3.8	
Co/Th	1.1	0.9	2.8	3.2	4.8	0.1	1.6	
Cr/Ni	2.7	2.1	1.9	2.0	7.6	10.3	1.9	
Cr/Th	5.8	5.3	10.5	11.4	12.1	0.8	7.8	
Cr/V	0.8	0.9	0.7	0.9	0.2	0.5	0.8	
Hf/Sc	0.2	0.2	0.3	0.3	0.6	0.8	0.4	
Cr/Zr	0.6	0.6	0.5	0.5	0.1	0.1	0.4	
La/Co	2.1	2.8	1.1	1.1	1.7	28.3	1.8	
La/Cr	0.4	0.5	0.3	0.3	0.7	2.2	0.4	
La/Y	1.2	1.7	1.3	1.4	0.7	1.1	1.4	
La/Yb	10.7	14.9	10.0	11.9	6.6	13.6	13.6	
La/Sc	1.9	2.2	1.6	1.7	1.3	5.7	2.2	
La/Sm	6.1	6.2	5.7	5.9	3.5	5.6	6.7	
La/Th	2.4	2.5	3.1	3.5	8.2	1.8	2.8	
Y/Ni	0.9	0.6	0.4	0.4	7.3	21.6	0.5	
$(La/Yb)_N$	7.21	10.07	6.71	8.01	4.44	9.14	9.21	
$(La/Sm)_N$	3.82	3.91	3.59	3.74	2.22	3.51	3.40	
$(Gd/Yb)_N$	1.28	1.58	1.25	1.32	1.53	1.81	1.39	
Eu/Eu*	0.69	0.64	0.73	0.79	1.03	0.2	0.65	
Σ REE	187.4	197.34	114.42	90.65	80.46	230.47	146.37	

Major element concentrations in weight percent and trace element concentrations in ppm, *LOI* loss of ignition, *d.l.* detection limit, *UCC* upper continental crust after McLennan (2001)

rocks, which is supported by the range of values of characteristic element ratios like Th/Sc (0.8–0.9), Eu/Eu* (0.64–0.69), Th/Co (0.9–1.1), La/Sc (1.9–2.3), Th/Cr (0.2) and La/Co (2.1–2.8) (Cullers 2000, 2002; Cullers and Podkovyrov 2002) and low concentrations of Cr and Ni (89–96 and 36–42 ppm, respectively). The immobile elemental ratios fit well when comparing chloritoid schists with the UCC. At the same time, those ratios differ considerably when comparing chloritoid schists and PsC chlorite schists (Table 1), implying a different provenance for those two low-grade rock types in the Kutjevačka Rijeka transect.

Mineral chemistry

The selected chemical analyses of chloritoid, chlorite (sorted as pairs for chloritoid–chlorite thermometry) and white mica are given in Table 2. The chemical criteria given by Vidal and Parra (2000) were used for selecting the EMP analyses of phyllosilicates (chlorite and white mica), separating the analyses suitable for further petrogenetic considerations.

The chloritoids show rather uniform composition when looking at the isolated domains in the analyzed samples. However, when comparing compositional variability

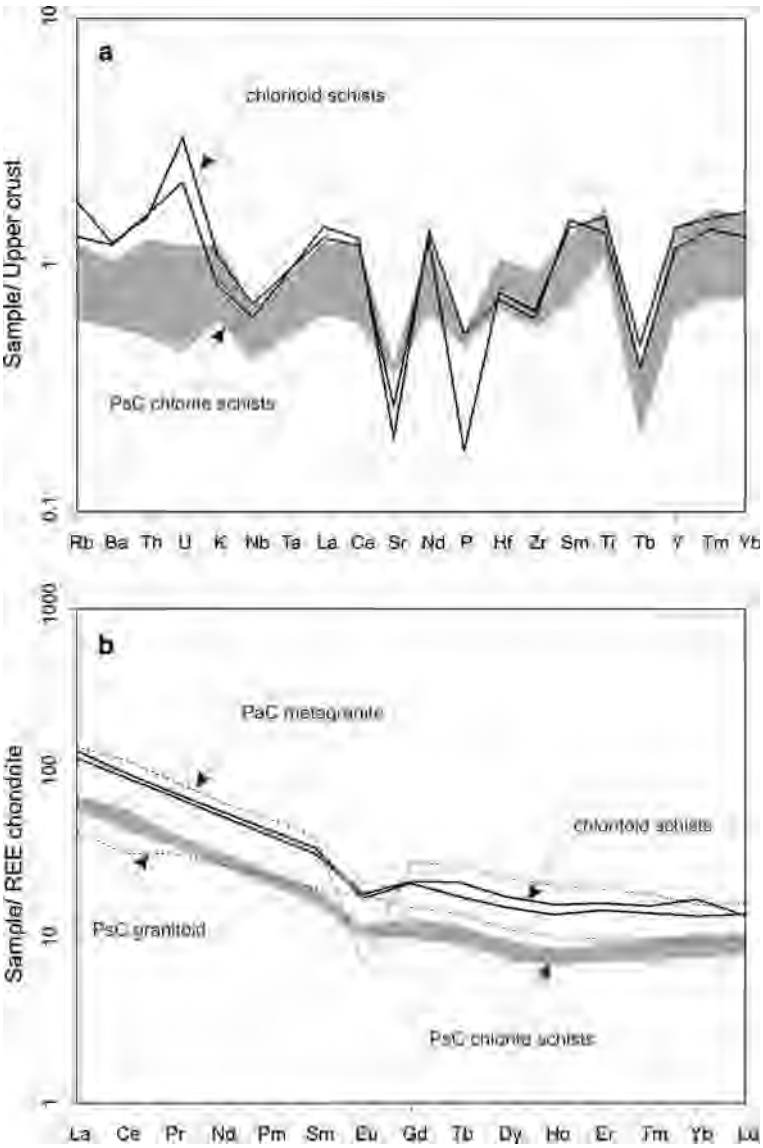

Fig. 3 **a** Upper Continental Crust (UCC)-normalized (Taylor and McLennan 1985) trace element composition. **b** Chondrite-normalized (Boynton 1984) rare earth element (REE) patterns of Kutjevačka Rijeka transect chloritoid schists and PsC chlorite schists. The PaC metagranite and PsC granitoid patterns are given as a reference

among chloritoids from different samples or different domains in the same outcrop, chemical variability resulting from the chemical heterogeneity of the protolith can be noted. The structural formula of chloritoid (Table 2) is calculated on the basis of 12 oxygens. The Si content is 2.1–2.2 apfu and consequently Al reaches 3.8–3.9 apfu. Fe^{3+} (0.07–0.25 pfu) and Mn (0.01–0.04 pfu) contents are uniformly low. The analyzed chloritoids are Fe-rich (Fe^{2+} 1.33–1.55 apfu, Mg 0.32–0.43 apfu,) with gradual slight decrease of Fe/(Fe + Mg) ratio from the cores (x(ctd) = 0.86–0.88) to the rims of the larger chloritoid grains (0.79–0.84). As stressed out by the microstructural analysis, chloritoids formed within the matrix, postdating S_2 foliation development; therefore, the observed chemical differences cannot be due to the different chemical composition of the microsystem in which the chloritoids nucleated and grew. This systematic variation has been interpreted as a result of the prograde metamorphic conditions prevailing during the growth of the chloritoids.

Microprobe analyses of chlorite grains in textural equilibrium with chloritoid which are selected for geothermometry are provided in Table 2. The number of cations is calculated on the basis of 14 oxygens. The Mn, Ti, Na and K contents of chlorites are practically negligible, with rather homogeneous compositions and very slight variations in x (chl) = Fe/Fe + Mg = 0.33–0.34, showing the Mg-rich nature of the chlorites. The Si content is 3.0–3.2 apfu, Al_{tot} content varies from 2.8 to 3.2, apfu while the number of tetrahedral aluminum atoms is 0.8–1.0 apfu.

The white micas are represented by optically hardly distinguishable association of newly formed (metamorphic)

Table 2 Selected microprobe analyses from the chloritoid schists mineral assemblage

	Chloritoid									
	Ctd 24a1	Ctd 24a2	Ctd 24a3	Ctd 24b1	Ctd 24a4	Ctd 24b2	Ctd 24b3	Ctd 24b4	Ctd 24a5	Ctd 24a6
SiO_2	24.31	24.22	24.53	27.34	24.98	27.00	27.82	28.60	26.84	27.98
TiO_2	0.18		0.18							
Al_2O_3	37.70	38.90	38.45	40.79	38.68	40.38	40.36	41.00	40.47	40.54
FeO	23.47	22.81	23.01	25.24	21.72	23.91	25.34	24.31	23.40	24.77
MnO	0.43	0.38	0.33		0.40	0.13	0.54	0.30	0.48	0.18
MgO	2.49	2.57	2.60	2.71	2.71	3.10	2.40	3.68	1.83	2.56
CaO		0.01								
Total	88.58	88.89	89.10	96.07	88.49	94.51	96.46	97.89	93.02	96.03
							Core	Rim	Core	Rim
Si	2.10	2.08	2.10	2.17	2.15	2.17	2.21	2.22	2.21	2.23
Ti	0.01		0.01							
Al	3.84	3.93	3.88	3.82	3.92	3.83	3.78	3.75	3.92	3.81
Fe^{3+}	0.15	0.07	0.11	0.18	0.08	0.17	0.22	0.25	0.08	0.19
Fe^{2+}	1.55	1.57	1.54	1.50	1.48	1.44	1.47	1.33	1.53	1.46
Mn	0.03	0.03	0.02	0.00	0.03	0.01	0.04	0.02	0.03	0.01
Mg	0.32	0.33	0.33	0.32	0.35	0.37	0.28	0.43	0.22	0.30
x(ctd)	0.84	0.83	0.83	0.82	0.82	0.81	0.86	0.79	0.88	0.84
Chl-Ctd pairs	Ctd 24a1	Ctd 24a2	Ctd 24a3	Ctd 24b1	Ctd 24a4	Ctd 24b2	Ctd 24b2			
Vidal et al. (1999)	Chl 24a1	Chl 24a1	Chl 24a1	Chl 24b1	Chl 24a1	Chl 24b2	Chl 24b1			
T (°C)	336	338	343	348	360	382	387			

	Chlorite				White mica			
	Chl 24a1	Chl 24b1	Chl 24b2		Mu 24a1	Mu 24a2	Mu 24a3	Mu 24a4
SiO_2	35.07	32.25	31.66		48.09	48.22	48.03	48.38
TiO_2					0.97	0.80	0.44	
Al_2O_3	26.03	28.81	29.02		34.82	34.61	34.43	34.92
FeO	14.57	14.60	13.93		0.04	1.13	1.39	0.91
MnO	0.03							
MgO	16.46	16.03	15.64		0.39	0.19	0.41	0.38
Na_2O					0.68	1.15	0.84	0.93
K_2O					9.35	9.30	8.92	8.71
Total	92.16	91.69	90.25		94.34	4.55	94.46	94.23
Si	3.20	2.98	2.96		6.36	6.35	6.37	6.40
Ti					0.10	0.08	0.04	0.00
Al IV	0.80	1.02	1.04		1.64	1.65	1.63	1.60
Al VI	2.00	2.12	2.16		3.78	3.72	3.75	3.85
Fe^{2+}	1.11	1.13	1.09			0.12	0.15	0.10
Mn								
Mg	2.24	2.21	2.18		0.08	0.04	0.08	0.07
Na					0.17	0.29	0.22	0.24
K					1.58	1.56	1.51	1.47
				t.i.c.	1.75	1.86	1.73	1.71
x(chl)	0.33	0.34	0.33	Na/(Na + K)	0.10	0.16	0.13	0.14
				P_1(GPa)	0.446	0.429	0.475	0.539
				P_2(GPa)	0.394	0.236	0.400	0.348

Cation numbers are calculated on the basis of 12 O for chloritoid, 22 O for white mica and 14 O for chlorite. Mineral abbreviations as in Fig. 5. Calculated temperatures are after Vidal et al. (1999) chlorite–chloritoid thermometer calibration, while pressure (P_1 and P_2) are obtained with calibrations after Coggon and Holland (2002) and Caddick and Thompson (2008); t.i.c. is total interlayer charge

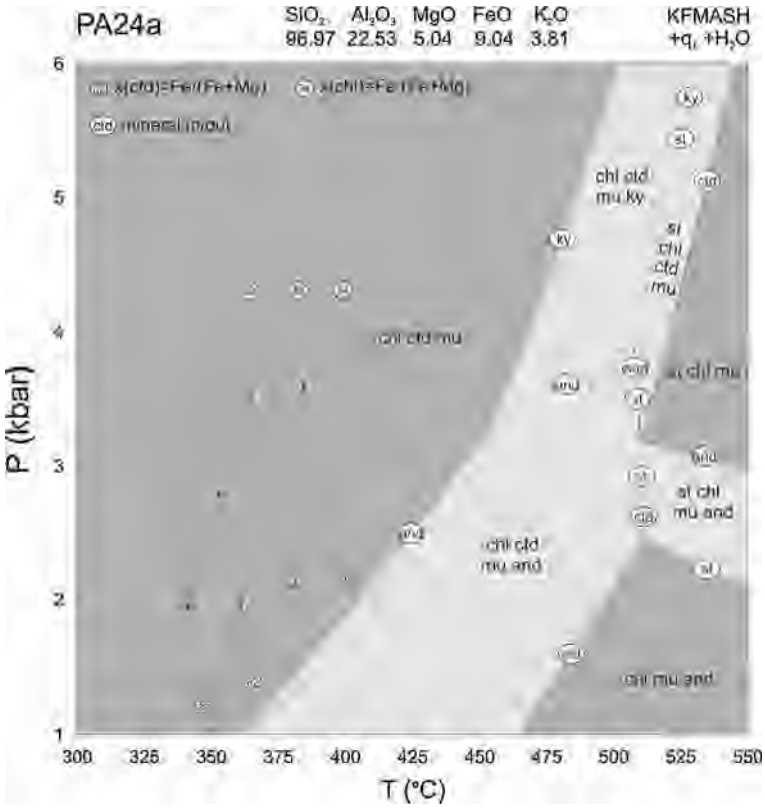

Fig. 4 Kutjevačka Rijeka transect chloritoid schist KFMASH pseudosection with chlorite and chloritoid isopleths and *P–T* conditions. *Dots* represent chlorite and chloritoid isopleth intersections, while concentric circles represent multiple identical *P–T* values. Mineral data are from Table 2. End member and other abbreviations after Holland and Powell (1990)

and authigenic micas giving the chemically variable and apparently non-equilibrated mixture, for the assemblage with chlorite and chloritoid. Since we could not apply, for example, TEM study in order to solve and clarify the nature of the micas, we applied chemical criteria like difference between layer and interlayer charges and K content for several white mica grains to select grains which are in equilibrium or near-equilibrium assemblage. However, such assumptions limited the use of the white micas in petrogenetic considerations.

White mica chemical composition (Table 2; calculated for 22 O) shows a deficiency in the interlayer cations K + Na = 1.71–1.86 apfu, Na/(Na + K) ratio 0.1–0.16. This deficit is characteristic of low-grade K-white micas (i.e., Árkai 2002; Árkai et al. 2003). The deficiencies in K and Na indicate moderate proportions of the pyrophyllite end member as already noted by Slovenec (1986) using XRD method. Due to small but significant deficit in the interlayer charge, the white micas are set mainly along the muscovite–phengite line, but being slightly shifted toward the illite field. The Si content ranges from 6.35 to 6.40 apfu, while the Mg + Fe sum ranges from 0.08 to 0.24 apfu. The Tschermak-type phengitic (or celadonitic) $^{IV}Al^{VI}_{-1}Al_{-1} = Si(Fe^{2+}, Mg)$ substitution predominates in the white micas. Ferric iron in white micas does not seem to be important, and there is no significant correlation between the Fe and Mg contents either.

Geothermobarometry

For individual geothermometric and geobarometric calculations, mineral compositions were selected from the domains of apparent textural equilibrium. Assuming that chlorite–chloritoid rims are in equilibrium, calculated *P–T* conditions correspond to the peak conditions of metamorphism that postdated the main folding event.

Chl–Ctd thermometry

The empirical chlorite–chloritoid calibration (Vidal et al. 1999) has been applied to the Kutjevačka Rijeka transect chloritoid schists. This thermometer is a Fe/Mg exchange thermometer for reaction Fe-chloritoid + Mg-chlorite = Mg-chloritoid + Fe-chlorite where partitioning of Fe and Mg between chlorite and chloritoid in equilibrium is given by the expression:

$$T(^{\circ}\mathrm{C}) = [1977.7/(\ln\ K_D + 0.971)] - 273.15,$$

where $K_D = (Fe/Mg)_{Ctd}/(Fe/Mg)_{Chl}$. K_D decreases and tends toward unity with increasing equilibrium temperature. This geothermometer is applicable for the temperature range from 300 to 500 °C, covering greenschist to blueschist facies conditions. It is also pressure independent and therefore can be used without prior information about the pressure of the metamorphism.

Application of Chl–Ctd thermometer to seven selected chlorite–chloritoid pairs (rim to rim) in textural equilibrium resulted in the temperature range of 336–387 °C (Table 2).

Phengite barometry

The pressure dependence of white mica Si content is well established (e.g., Massonne and Schreyer 1987). Testing of the phengite model in numerous subsystems (KFASH, KMASH, NKASH and NKMASH) was discussed by Coggon and Holland (2002) and Caddick and Thompson (2008) and yields simple barometer expression:

$$P(\mathrm{GPa}) = 4.19\mathrm{Si}_{\mathrm{Phe}} + 0.0036T(\mathrm{K}) - 15.15.$$

Due to Tschermak substitution, Si content is coupled with the strongly *P–T* dependent Mg content, and the expression can be written as

$$P(\mathrm{GPa}) = 8.35\mathrm{Mg}_{\mathrm{Phe}} - 1.72\mathrm{Si}_{\mathrm{Phe}} + 0.0015T(\mathrm{K}) + 4.59.$$

Using the calibrations given above for an estimated average temperature of 360 °C, obtained pressure values are in the range 4.3–5.4 kbar for Si content and 2.4–4 kbar for Si coupled with Mg content, respectively. The graphical approach for Massonne and Schreyer (1987) pressure–temperature plot with Si isopleths in the limiting assemblage indicates approx. 3.5–4 kbar at 360 °C. The obtained results regarding the observed assemblages should be treated as minimum pressure values.

KFMASH pseudosection geothermobarometry using Chl–Ctd isopleths

The simple mineral assemblage allows the use of model system KFMASH (K_2O–FeO–MgO–Al_2O_3–SiO_2–H_2O). For the bulk composition of sample PA24a (molar amounts SiO_2:Al_2O_3:MgO:FeO:K_2O = 96.97:22.53:5.04:9.04:3.81), pseudosection with quartz and H_2O in excess have been calculated (Fig. 4). The pseudosection covers the *P–T* range of 300–550 °C and 1–6 kbars for the different phase equilibrium assemblages including observed assemblage ctd + chl + mu (+q + H_2O).

The largest field is occupied by the observed ctd + chl + mu (+q + H_2O) assemblage at whole *P* range and low temperatures. The assemblage stability at low pressures is around 350 °C while at 6 kbar it reaches temperatures up to 475 °C. Chloritoid itself is stable up to 460 °C at low pressures and 550 °C at medium pressures, while chlorite stability is just over the temperatures of 550 °C for the whole *P* range. Staurolite stability field just precedes the chloritoid-out line. Note in particular that kyanite stability extends to low pressures and moderate temperatures, and garnet is not stable at all in the calculated *P–T* field.

Isopleths representing measured compositions of chloritoid and chlorite pairs from sample PA24a intersect in the chloritoid + chlorite + muscovite field at approximately 340–385 °C and 1.95–3.6 kbar. These *P–T* data match well with the data obtained by the other geothermobarometric methods.

Xenotime age dating

One prospective way to determine the metamorphic age of a low-grade metapelitic series is to search for accessory monazite and/or xenotime grains, in order to date these by means of the electron microprobe, based on their Th–U–Pb contents (Suzuki et al. 1991; Montel et al. 1996). Many studies suggest that both monazite and xenotime form in metapelites already at low-grade metamorphic conditions (e.g., Overstreet 1967; Finger et al. 2002; Rasmussen and Muhling 2007; Rasmussen et al. 2010; Janots et al. 2008). Additionally, metapelites may contain pre-metamorphic monazite or xenotime, either as detrital relics or as authigenic, diagenetic minerals (e.g., Kositcin et al. 2003; Vallini et al. 2005; Hetherington et al. 2008; Krenn et al. 2008).

Several polished thin sections of the chloritoid schists have been examined by the microprobe for accessory monazite or xenotime, using backscatter electron imaging techniques. No monazite could be encountered. However, small xenotime grains, 10–30 μm in size, could be detected. Unfortunately, the Th and U contents of these xenotime grains were in most cases below 0.3 wt%, permitting no reasonable age dating due to too low radiogenic Pb contents. In one sample, xenotimes with somewhat higher U and radiogenic Pb contents were found and were subjected to xenotime dating. Texturally and in modal content, this sample does not distinguish from other samples of the chloritoid schists. It contains approximately 10 vol.% of euhedral chloritoid laths, most of them being 0.2–0.5 mm long. They are embedded in a fine-grained foliated groundmass of white mica, quartz and chlorite.

Most of the tiny xenotime grains are irregularly distributed within the white mica–quartz–chlorite matrix. A few xenotime grains are enclosed within the chloritoid crystals (Fig. 5). BSE imaging at high magnification reveals that actually all xenotime grains are chemically zoned. Many grains exhibit thin outer seams with a bright BSE signal (Fig. 5c, e). These seams appear to represent the youngest phase of xenotime formation in the rock. Additionally, distinct core domains representing the early stages of xenotime growth can sometimes be delineated in the BSE images.

Th–U–Pb ages and their errors were calculated according to Montel et al. (1996). To control the quality of the dating results, several xenotime age standards (30, 350 and

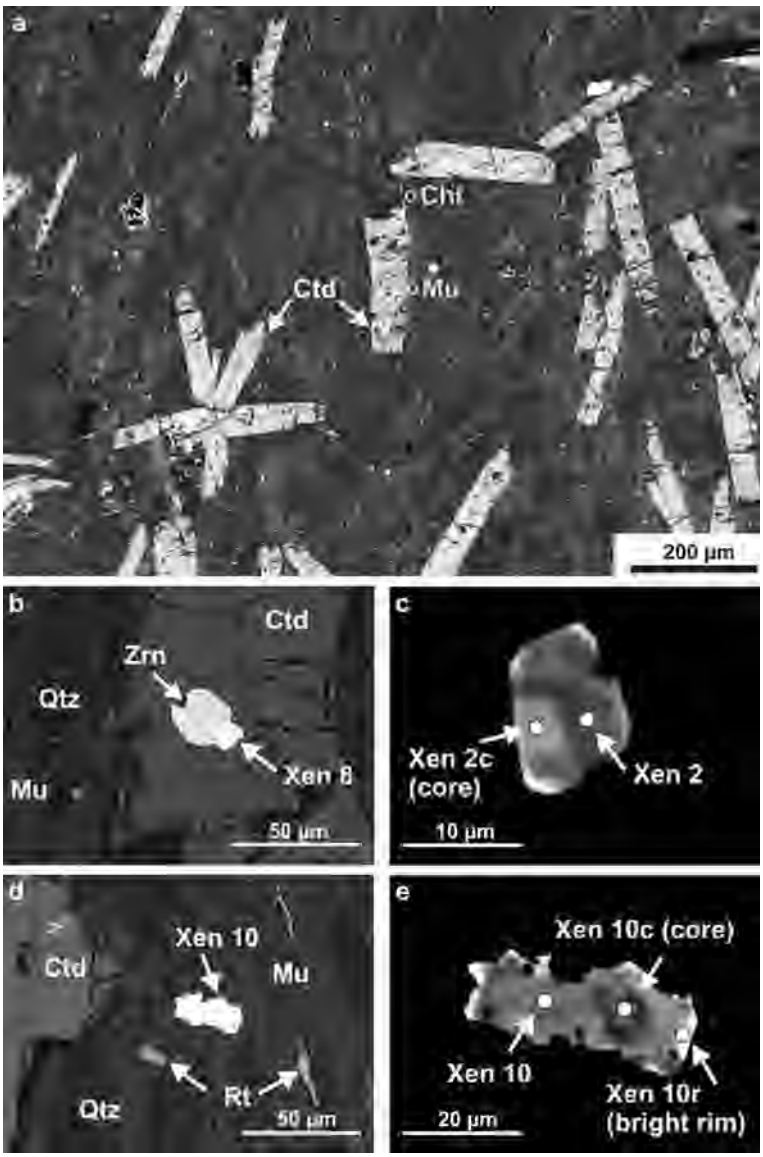

Fig. 5 BSE images of chloritoid schist showing the typical mineral assemblage ctd–chl–mu–qtz; **a** single idiomorphic, lath-shaped chloritoid grains and chloritoid rosettes; **b–e** examples of accessory xenotime grains, note the striking compositional heterogeneity of the individual grains at high magnification. Abbreviations: *Chl* chlorite, *Ctd* chloritoid, *Mu* white mica (muscovite), *Qtz* quartz, *Zrn* zircon, *Xen* xenotime, *Rt* rutile

920 Ma) were measured under the same conditions as the specimen. In all cases, the recommended age values could be reproduced within the particular error ranges (±30 Ma or better).

Representative microprobe analyses of the accessory xenotimes are listed in Table 3. While the Y_2O_3 contents of all measured xenotime grains turned out to be fairly constant (39–46 wt%), a surprisingly strong variation is observed for the Gd_2O_3 (1.7–10.7 wt%) and Yb_2O_3 (2.9–7.9 wt%). Figure 6 shows that there is a strict negative correlation between Gd and Yb. Analyses of the core domains of xenotimes generally yielded the lowest Gd and highest Yb contents, while the analyses within the bright xenotime seams gave the highest Gd and lowest Yb contents. Obviously, a systematic increase in HREE/MREE occurred with time. Although the U content of the xenotimes also shows a considerable variation (0.1–1.5 wt%), it appears to be uncorrelated to the Gd/Yb trend (Fig. 6b). The highest U contents were recorded in the domains with the intermediate Gd/Yb ratios, that is, mostly in positions halfway between cores and rims. Th (0.01–0.31 wt%) is always lower than U.

Six analysis spots with U > 0.3 wt% had Pb contents in a measurable range and could be used to calculate the formation ages (Table 3). Five of these analyses gave consistently Th–U–Pb ages between 72 ± 56 and 154 ± 72 Ma (Cretaceous to Upper Jurassic). The data overlap within error and indicate a formation of the dominating metamorphic imprint in the rocks during the Alpine event (weighted average age of the five analyses: 120 ± 36 Ma). Data distribution in a U* versus Pb isochron diagram (Suzuki and Adachi 1991) follows an

Table 3 Representative microprobe analyses for xenotime from chloritoid schist

	Xen 2 c in matrix	Xen 2 in matrix	Xen 3 in matrix	Xen 4 in matrix	Xen 6 in matrix	Xen 8 in Ctd	Xen 10 c in matrix	Xen 10 in matrix	Xen 10 r in matrix
SiO_2	0.06	0.07	0.08	0.12	0.00	0.20	0.23	0.01	b.d.l.
P_2O_5	35.70	35.75	35.45	35.26	34.95	35.01	35.27	35.48	35.09
CaO	0.02	0.05	0.05	0.22	0.13	0.10	0.02	0.08	b.d.l.
Y_2O_3	45.58	44.88	45.55	43.30	43.24	44.09	45.94	44.90	39.40
Nd_2O_3	0.14	0.23	0.11	0.22	0.38	0.30	0.10	0.31	0.54
Sm_2O_3	b.d.l.	0.42	b.d.l.	0.55	0.64	0.47	b.d.l.	0.51	0.68
Gd_2O_3	1.76	4.08	2.47	5.59	4.78	4.62	2.96	4.60	10.71
Dy_2O_3	3.07	5.51	4.06	6.38	5.92	5.87	4.75	5.82	7.87
Er_2O_3	5.49	4.48	4.92	3.67	4.19	4.16	5.02	4.27	3.00
Yb_2O_3	7.92	4.30	5.93	3.55	4.13	4.08	4.62	3.85	2.95
ThO_2	0.02	0.14	0.01	0.31	0.13	0.12	0.06	0.03	0.18
UO_2	0.26	0.66	0.32	0.83	0.37	1.52	0.86	0.91	0.09
PbO	b.d.l.	b.d.l.	0.04	0.02	0.01	0.03	0.03	0.01	b.d.l.
SO_3	b.d.l.	0.01	0.02	0.02	b.d.l.	0.02	0.02	0.02	b.d.l.
Total	100.03	100.58	99.02	100.06	98.86	100.57	99.88	100.81	100.52
Si	0.002	0.002	0.003	0.004	0.000	0.007	0.008	0.000	0.000
P	1.004	1.005	1.004	1.003	1.005	0.995	0.996	1.001	1.012
Ca	0.001	0.002	0.002	0.008	0.005	0.003	0.001	0.003	0.000
Y	0.805	0.793	0.811	0.774	0.782	0.787	0.815	0.796	0.715
Nd	0.002	0.003	0.001	0.003	0.005	0.004	0.001	0.004	0.007
Sm	0.000	0.005	0.000	0.006	0.007	0.005	0.000	0.006	0.008
Gd	0.019	0.045	0.027	0.062	0.054	0.051	0.033	0.051	0.121
Dy	0.033	0.059	0.044	0.069	0.065	0.063	0.051	0.062	0.086
Er	0.057	0.047	0.052	0.039	0.045	0.044	0.053	0.045	0.032
Yb	0.080	0.044	0.061	0.036	0.043	0.042	0.047	0.039	0.031
Th	0.000	0.001	0.000	0.002	0.001	0.001	0.000	0.000	0.001
U	0.002	0.005	0.002	0.006	0.003	0.011	0.006	0.007	0.000
Pb	0.000	0.000	0.000	0.000	0.000	0.000	0.000	0.000	0.000
S	0.000	0.000	0.001	0.000	0.000	0.000	0.001	0.000	0.000
Tetr.	1.002	1.002	1.003	1.001	0.999	0.996	0.999	0.995	1.004
A[8]	0.996	0.997	0.996	1.000	1.002	1.006	1.002	1.007	0.993
Age dating results									
Th	0.015	0.120	0.012	0.273	0.111	0.103	0.054	0.029	0.155
U	0.225	0.584	0.281	0.733	0.322	1.343	0.761	0.803	0.081
Pb	b.d.l.	0.014	b.d.l.	0.017	0.006	0.023	0.024	0.008	b.d.l.
U*		0.622		0.818	0.357	1.375	0.777	0.812	
Age (Ma)		154		148	115	121	219	72	
$\pm 2\sigma$		72		55	126	33	81	56	

U* values calculated according to Suzuki and Adachi (1991). Values are in wt%. Formula recalculation on the basis of 4 O; b.d.l.—below detection limit

isochron (Fig. 7), implying the ages are trustworthy and not significantly influenced by the common Pb presence. It is important to note that the Alpine age was determined in xenotime domains with intermediate Gd/Yb ratios, positioned half way between core and rim of the grain. The sixth analysis, in a high-Yb core domain, gave a slightly greater age of 219 ± 81 Ma, the significance of which remains unclear. Unfortunately, we were not successful in the attempt to date other Yb-rich cores, because the Pb content was always below the detection limit. Likewise, the small Gd-enriched rims of the xenotime were not datable, as the Pb content was generally below the detection limit.

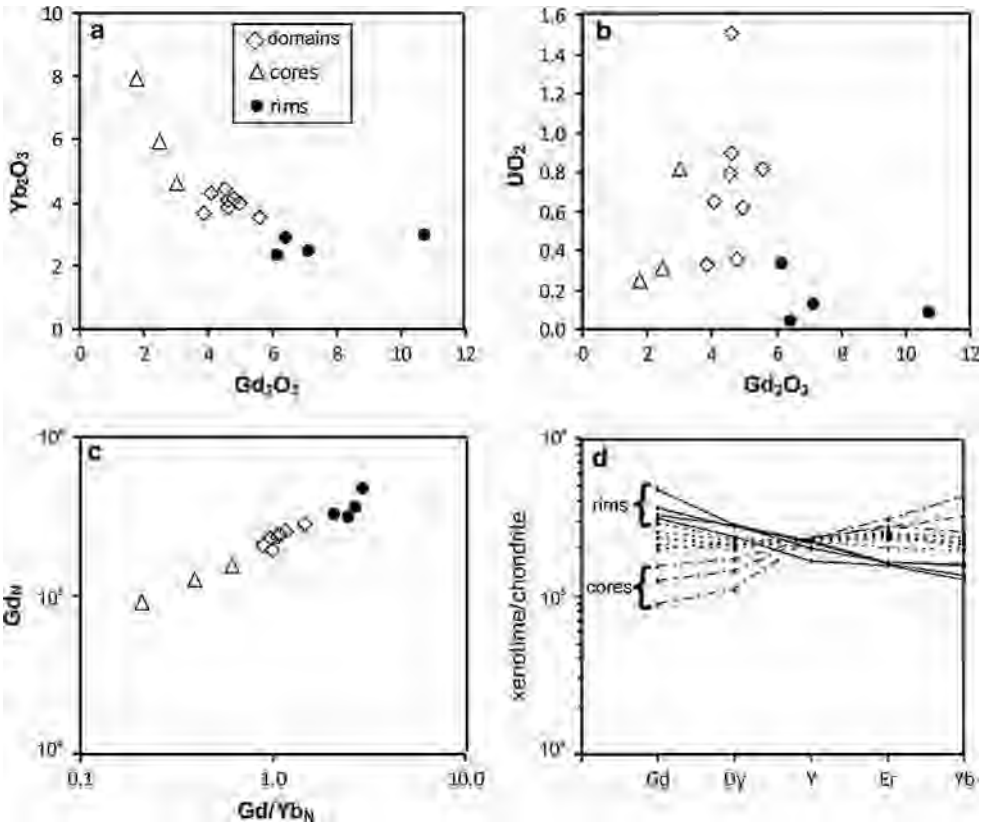

Fig. 6 Chemical diagrams illustrating the compositional variation of xenotime in chloritoid schists. Values in **a** and **b** are weight percent oxides. Values in **c** and **d** are normalized to chondrite, using chondrite data from Anders and Grevesse (1989). *Diamond* symbols represent domains with intermediate Gd/Yb ratios

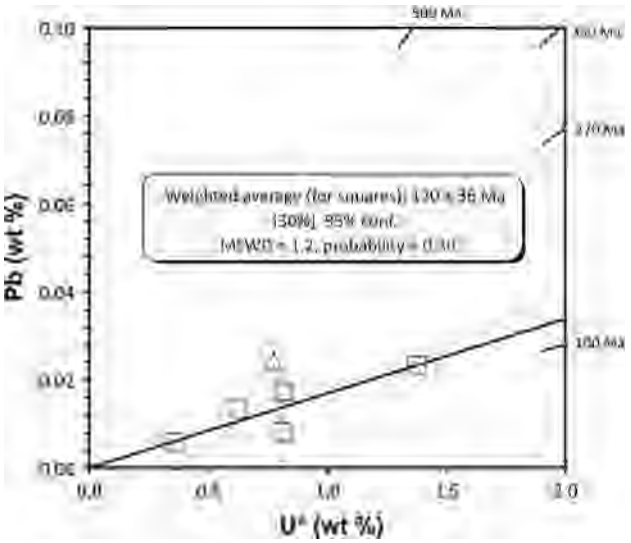

Fig. 7 U* versus Pb isochron diagram after Suzuki and Adachi (1991) with data for xenotime from chloritoid schists (see Table 3). Shown isochron refers to the weighted average age of 120 ± 36 Ma and is forced through zero. Age scale refers to zero-intersect isochrons

Discussion

Looking at the large-scale paleogeographic reconstructions in the timeframe between Variscan and Alpine orogenies, polymetamorphic complexes of Tisia belonged to the southern margin of the European plate. The Slavonian Mts. (Papuk), together with the nearby Villány area occupied the most external position within Tisia, toward the Neotethys (Golonka 2004; Schmid et al. 2008). Following the Variscan orogeny, post-orogenic mollase-type sedimentation produced a non-metamorphic sedimentary cover over the eroded surface of the crystalline basement. The Slavonian Mts. sedimentary cover contains a Late Carboniferous flora (Westphalian; Brkić et al. 1974) in its middle part as the only paleontological evidence of its depositional age. The younger and older parts of Late Paleozoic sedimentary cover tend to be devoid of any paleontological record, making the precise determination of the onset of sedimentation together with the whole depositional age span based on biostratigraphy impossible. That leaves us with a quite wide and uncertain time frame for the onset of sedimentation, including the one of the protolith of chloritoid schists, in range from the crystallization of the most probable source material (than cooling, uplift and erosion) to the age of the Westphalian flora (minus age span needed for deposition of approx. 1,000 m thick (meta) sedimentary sequence).

Origin of detrital source material

Due to their relatively immobile nature, the distribution of selected trace elements, such as Th, Sc, Zr, Hf, REE, Cr, V,

Ni together with trace elements ratios like La/Sc, La/Co, La/Th, Co/Th, Th/Sc, Cr/Th, Cr/Zr, is particularly useful indicators of geological processes, provenance and tectonic setting of psammitic and even to fine-grained sediments (Cullers 1994a, b). The REE, Th and Sc are the most useful for inferring source rock composition because they are not severely affected by diagenesis and low-grade metamorphism (Bhatia and Crook 1986; McLennan and Taylor 1991; Cullers 1995, 2002; Cullers and Podkovyrov 2002).

The chloritoid schists have higher TiO_2, Th, U, Y, Zr, Hf and REE contents relative to the underlying PsC chlorite schists (Table 1). Chondrite-normalized REE patterns, Th/Sc, La/Sc and La/Yb ratios and Cr, V, Ni contents are comparable to the UCC values. REE pattern of chloritoid schists displays light REE (LREE) enrichment trend, pronounced negative Eu anomaly ($Eu/Eu^* = 0.64–069$) and nearly flat heavy REE (HREE) pattern. Typically, siliciclastic sediments derived from the mature continental crust are characterized by LREE enrichment and high ΣREE values. The low HFSE concentrations provide no support for the presence of significant amounts of mafic or ultramafic rocks in the source area. Geochemical characteristics of the chloritoid schists (Table 1) indicate that detrital material (i.e., protolith of chloritoid schists) has been produced primarily from the exposed upper crustal material and that felsic rocks dominated in the source area.

The idea that the source material had a local origin (from PsC to PaC) was already presented by Jamičić (1988). Such idea is additionally supported by geochemical and provenance studies in the neighboring Upper Paleozoic sedimentary complexes of Tisia in Mecsek and Villány area (Varga and Szakmány 2004; Varga et al. 2007) which concluded that source rocks for those complexes were felsic igneous rocks, that is, upper crustal material. Also, their geotectonic setting has been related to an active margin (continental island arc/active continental margin settings).

Geochemistry of analyzed chloritoid schists, in comparison with the metamorphic rocks of the older PsC (chlorite schists), points to a conclusion that differences in the immobile element signatures are the consequence of derivation of these rocks from different sources. Generally, sediments derived from young undifferentiated oceanic arcs have lower $(La/Sm)_N$ ratios than either continental arc or old continental crust, also show lower ΣREE value and the lack of Eu anomaly, which is consistent with the observed pattern of typical PsC rocks.

Taking into consideration the geochemical characteristics of chloritoid schists presented here, together with geology and geochemistry of representative rocks from the surrounding area, the best candidate that could have given the protolith is felsic (granitoid and gneissic) rocks that outcrop in the Papuk Complex. However, this geochemical consistency with PaC does not rule out provenance from another similar, previously existing, granitoid massif but implies the most probable source.

Formation of chloritoids

Fe-chloritoid generally occurs in low- to medium-grade metamorphic rocks, plotting in a restricted field of bulk compositions (Hoschek 1967) characterized by low alkali abundances, $(FeO + MgO)/(FeO + MgO + Al_2O_3) < 0.63$ and $FeO/(FeO + Al_2O_3) < 0.58$. The analyzed chloritoid schists show average values of 0.27–0.34 and 0.22–0.28 for these two ratios, respectively. The post-tectonic character of chloritoid with respect to S_2 foliation shows that its formation occurred after the major folding of the HSC. Chloritoid should be related to the peak thermal (metamorphic) conditions and prograde reactions on the earlier non- to anchi-metamorphic assemblages. The following Hoschek's (1969) chloritoid-in reaction

$$\text{Chlorite} + \text{AlSiO}_x\,(\text{kaolinite} + \text{pyrophyllite}) = \text{chloritoid} + \text{quartz} + H_2O$$

can be considered as the reaction responsible for the generation of chloritoid. This reaction is stable just below the temperature of 400 °C. Chloritoid appears in metapelites in the KFMASH system at about 300–350 °C and can be stable up to 550 °C (Spear 1993), and it is considered as a typical epizonal index mineral (>300 °C). Absence of staurolite and garnet indicates that the upper boundary of chloritoid stability field, that is, the breakdown of chloritoid to garnet and staurolite in the presence of quartz, has not been reached. Consistent with experimental investigations and natural occurrences of chloritoid-bearing rocks, the lack of garnet in the assemblage suggests that metamorphic temperatures were well below ca. 550 °C. The presence of chlorite in the assemblage limits the upper thermal stability. Following Hoschek's (1969) paper, Vragović and Majer (1979a) concluded that assemblage of chloritoid and chlorite is stable at temperatures around 400 °C for Slavonian chloritoid schists. Stability of a third mineral in the assemblage, K-deficient white mica in coexistence with pyrophyllite is in the temperature range 300 to approx. 360 °C in natural assemblages (Rosenberg 2002). The lack of kyanite can be explained in a similar manner in respect to pressure limitations imposed by the presence or absence of assemblage containing kyanite which will not be stable below 450 °C at low pressures of 3–4 kbars.

Temperatures calculated with chl–ctd thermometer of Vidal et al. (1999), phengite barometry (Massonne and Schreyer 1987) and isopleths intersections in the KFMASH pseudosection (3.5–4 kbar and 340–380 °C) correspond

well to the expected temperature and pressure values for the stability of the observed mineral assemblage.

Interpretation of xenotime age data

Our attempt to constrain the metamorphic age of the chloritoid schists on the basis of chemical xenotime dating yielded only a partial success. Formation ages could have been calculated only for a selection of U-enriched xenotime domains, while the bulk of accessory xenotime grains could not be dated as a consequence of too low U, Th and radiogenic Pb contents. Nevertheless, it is clear from the available dating results on the U-enriched grains that the xenotime population of the chloritoid schist cannot be interpreted as entirely Variscan or older. A substantial part of the xenotimes must have formed during low-grade metamorphism related to the Alpine orogenic cycle, suggesting that the low-grade metamorphic mineral paragenesis in the rock unit (with chloritoids) is related to the Alpine orogenic cycle. This interpretation is also strongly supported by the fact that a xenotime with an age value of 121 ± 33 Ma was found as an inclusion inside the chloritoid (grain 8 in Table 3). Conversely, only one spot analysis in a xenotime core (Xen 10c in Table 3) provided evidence for a possible presence of older xenotime.

Based on the findings of Vallini et al. (2005) for xenotime from a low-grade metasedimentary sequence from SW Australia, it can be speculated that the Yb-rich cores of the Kutjevačka Rijeka chloritoid schist xenotime could be of detrital or diagenetic origin. In Vallini et al. (2005) example, Yb-rich xenotime cores formed during the diagenetic stage, while younger, low-grade metamorphic (hydrothermal) xenotime was found to be significantly enriched in Gd. It is possible that a similar interpretation may hold true for the composite xenotime in the chloritoid schist under the study, that is, that the Yb-rich cores may be diagenetic xenotime. Although low-grade metamorphic origin of the Yb-rich cores due to presence of two older foliations in the rock cannot be completely excluded, leaving relation between the age of foliation(s) and the core domains of xenotimes in the chloritoid schists open to discussion. We conjecture that the bulk of the xenotime grains, which are characterized by intermediate Gd/Yb ratios, formed prograde during Alpine (Cretaceous) low-grade metamorphic event. The Gd-enriched outer seams of the xenotime may be best explained as being of late-metamorphic hydrothermal origin.

Combined geochronological and thermobarometric data obtained from the crystalline rocks of the Tisia Mega-Unit in southern Hungary indicate that these Variscan rocks underwent Permian and Alpine metamorphic overprints (Horváth and Árkai 2002; Lelkes-Felvári et al. 1996, 2003; Horváth 2007). Árkai et al. (2000) outlined the Alpine metamorphism of the post-Variscan (Paleozoic and Mesozoic) cover sequences in the Tisia Mega-Unit. In the Slavonian Mts. in Croatia, a polyphase pre-Variscan and Variscan tectono-metamorphic evolution of the crystalline rocks have also been documented by structural, geochronological and thermobarometric studies (Jamičić 1983, 1988; Pamić and Lanphere 1991; Balen et al. 2006; Horváth et al. 2010), and recently supplemented by additional data indicating the thermal overprint during Cretaceous (Biševac et al. 2010).

The obtained Th–U–Pb age 120 ± 36 Ma is definitively related to the Alpine orogeny and can be tentatively attributed to one of the Late Mesozoic regional events important to the evolution of Tisia, like: (a) separation of the Tisia from the European continent, related to the opening of the Alpine Tethys during Jurassic (Bathonian; 168–165 Ma); (b) beginning of significant shifting of Tisia away from Europe, accompanied by complex rotations and translations (~130 Ma) together with Valangian to Barremian volcanism in Mecsek area; 3) sequence of nappe-stacking events, that is, extensive thrusting during Turonian; 94–89 Ma—(Márton 2000; Schmid et al. 2008; Ustaszewski et al. 2010).

Conclusions

1. The sedimentary protolith of chloritoid schists is derived mainly from felsic rocks of the upper continental crust. Following previous work of Jamičić (1988) implying the local source, geochemical data presented here plausibly (but not exclusively) relate source to the nearby Papuk Complex composed of granites, migmatites and gneisses of Variscan age. The protolith of the underlying Psunj Complex chlorite schists shows different characteristics and consequently a different source compared to chloritoid schists.
2. Peak metamorphic conditions during prograde growth of chloritoid from the Kutjevačka Rijeka transect chloritoid schists reached on average 3.5–4 kbar and 340–380 °C.
3. Obtained Th–U–Pb ages averaging 120 ± 36 Ma may be attributed to a Upper Jurassic to Cretaceous xenotime forming event, clearly indicating the Alpine orogeny.
4. Development of S_{0-1} and S_2 foliations comprising chlorite, white mica and quartz, together with a xenotime core dated at 219 ± 81 Ma, leaves an open possibility for the presence of older (pre-Alpine?) low-grade metamorphic phase.
5. Post-tectonic growth of chloritoid with respect to S_2 foliation indicates that the major phase of Alpine deformation predates the peak metamorphic conditions (thermal climax).

6. The prograde Alpine low-grade metamorphic event recorded in the growth of chloritoid can be tentatively related to the extensive regional metamorphism which appears to be the record of thermotectonic event(s) associated with the onset of Early to mid-Cretaceous ($\sim$130 Ma) substantial rotations and translations of Tisia from Europe or/and contemporaneous crustal shortening recorded in the Dacia and ALCAPA.

Acknowledgments The authors would like to thank Ralf Schuster for his helpful and constructive comments. This research was supported by Croatian Ministry of Science, Education and Sports grant 119-1191155-1156. The field and laboratory work were partly covered by bilateral (Austria–Croatia and Croatia–Hungary) scientific cooperation programs (project leaders F. Finger and D. Balen and D. Balen and P. Árkai/P. Horváth, respectively). Mrs. Zorica Petrinec is gratefully acknowledged for her help during preparation of manuscript.

References

Anders E, Grevesse N (1989) Abundances of the elements: meteoritic and solar. Geochim Cosmochim Acta 53:197–214

Árkai P (2002) Phyllosilicates in very low-grade metamorphism: transformation to micas. Rev Mineral Geochem 46:463–478

Árkai P, Bérczi-Makk A, Balogh K (2000) Alpine low-T prograde metamorphism in the post-Variscan basement of the Great Plain, Tisza Unit (Pannonian Basin, Hungary). Acta Geol Hung 43: 43–63

Árkai P, Faryad SW, Vidal O, Balogh K (2003) Very low-grade metamorphism of sedimentary rocks of the Meliata unit, Western Carpathians, Slovakia: implications of phyllosilicate characteristics. Int J Earth Sci 92:68–85

Balen D, Horváth P, Tomljenović B, Finger F, Humer B, Pamić J, Árkai P (2006) A record of pre-Variscan Barrovian regional metamorphism in the eastern part of the Slavonian Mountains (NE Croatia). Mineral Petrol 87:143–162

Belak M (2005) Metamorfne stijene facijesa plavih i zelenih škriljavaca na Medvednici (Metamorphic rocks of the blueschist and greenschist facies on the Medvednica Mt.). PhD thesis, University of Zagreb, pp 295 (in Croatian)

Bhatia MR, Crook KAW (1986) Trace element characteristics of graywackes and tectonic setting discrimination of sedimentary basins. Contrib Mineral Petrol 92:181–193

Biševac V, Balogh K, Balen D, Tibljaš D (2010) Alpine (Cretaceous) very low- to low-grade metamorphism recorded on the illite-muscovite-rich fraction of metasediments from South Tisia (eastern Mt Papuk, Croatia). Geol Carpathica 61:469–481

Boynton WV (1984) Geochemistry of the rare earth elements: meteorite studies. In: Henderson P (ed) Rare earth element geochemistry. Elsevier, Amsterdam, pp 63–114

Brkić M, Jamičić D, Pantić N (1974) Karbonske naslage u Papuku (sjeveroistočna Hrvatska) (Carboniferous deposits in Mount Papuk (northeastern Croatia)). Geol vjesnik Zagreb 27:53–58 (in Croatian)

Caddick MJ, Thompson AB (2008) Quantifying the tectono-metamorphic evolution of pelitic rocks from a wide range of tectonic settings: mineral compositions in equilibrium. Contrib Mineral Petrol 156:177–195

Chopin C (1983) Magnesiochloritoid, a key-mineral for the petrogenesis of highgrade pelitic blueschists. Bull Mineral 106:715–717

Chopin C (1985) Les relations de phases dans les metapelites de haute pression. PhD thesis, Université Pierre et Marie Curie, Paris, pp 80

Chopin C, Monié P (1984) A unique magnesiochlortoid-bearing, high-pressure assemblage from the Monte Rosa, Western Alps: petrologic and ^{40}Ar-^{39}Ar radiometric study. Contrib Mineral Petrol 87:388–398

Coggon R, Holland TJB (2002) Mixing properties of phengitic micas and revised garnet-phengite thermobarometers. J Metamorph Geol 20:683–696

Csontos L (1995) Tertiary tectonic evolution of the Intra-Carpathian area: a review. Acta Vulcanol 7:1–13

Csontos L, Vörös A (2004) Mesozoic plate tectonic reconstruction of the Carpathian region. Palaeogeogr Palaeoclimatol Palaeoecol 210:1–56

Cullers RL (1994a) The chemical signature of source rocks in size fractions of Holocene stream sediment derived from metamorphic rocks in the wet mountains region, Colorado, USA. Chem Geol 113:327–343

Cullers RL (1994b) The controls on the major-and trace-element variation of shales, siltstones and sandstones of Pennsylvanian-Permian age from uplifted continental blocks in Colorado to platform sediments in Kansas, USA. Geochim Cosmochim Acta 58:4955–4972

Cullers RL (1995) The controls on the major- and trace-element evolution of shales, siltstones and sandstones of Ordovician to Tertiary age in the Wet Mountains region, Colorado, USA. Chem Geol 123:107–131

Cullers RL (2000) The geochemistry of shales, siltstones and sandstones of Pennsylvanian-Permian age, Colorado, USA: implications for provenance and metamorphic studies. Lithos 51:181–203

Cullers RL (2002) Implications of elemental concentrations for provenance, redox conditions, and metamorphic studies of shales and limestones near Pueblo, CO, USA. Chem Geol 191:305–327

Cullers RL, Podkovyrov VN (2002) The source and origin of terrigenous sedimentary rocks in the Mesoproterozoic Ui group, southeastern Russia. Precambr Res 117:157–183

Finger F, Krenn E, Riegler G, Romano S, Zulauf G (2002) Resolving Cambrian, Carboniferous, Permian and Alpine monazite generations in the polymetamorphic basement of the eastern Crete (Greece) by means of the electron microprobe. Terra Nova 14:233–240

Fodor L, Csontos L, Bada G, Györfi I, Benkovics L (1999) Tertiary tectonic evolution of the Pannonian Basin system and neighbouring orogens: a new synthesis of palaeostress data. In: Durand D, Jolivet L, Horváth F, Séranne M (eds) The Mediterranean basins: tertiary extension within the Alpine Orogen, vol 156. Geol Soc London Spec Publ, pp 295–334

Géczy B (1973) The origin of Jurassic faunal provinces and the Mediterranean plate tectonics. Annales Universitatis Scientiarum Budapestinensis de Rolando Eötvös Nominatae, Sectio Geologica 16:99–114

Golonka J (2004) Plate tectonic evolution of the southern margin of Eurasia in the Mesozoic and Cenozoic. Tectonophysics 381: 235–273

Hetherington CJ, Jercinovic MJ, Williams ML, Mahan K (2008) Understanding geologic processes with xenotime: composition, chronology, and a protocol for electron probe microanalysis. Chem Geol 254:133–147

Holland TJB, Powell R (1990) An enlarged and updated internally consistent thermodynamic dataset with uncertainties and correlations: the system K_2O–Na_2O–CaO–MgO–MnO–FeO–Fe_2O_3–Al_2O_3–TiO_2–SiO_2–C–H_2–O_2. J Metamorph Geol 8:89–124

Holland TJB, Powell R (1998) An internally consistent thermodynamic dataset for phases of petrological interest. J Metamorph Geol 16:309–343

Holland TJB, Baker JM, Powell R (1998) Mixing properties and activity-composition relationships of chlorites in the system $MgO–FeO–Al_2O_3–SiO_2–H_2O$. Eur J Mineral 10:395–406

Horváth P (2007) P-T pseudosections in KFMASH, KMnFMASH, NCKFMASH and NCKMnFMASH systems: a case study from garnet-staurolite mica schist from the Alpine metamorphic basement of the Pannonian Basin (Hungary). Geol Carpathica 58:107–119

Horváth P, Árkai P (2002) Pressure–temperature path of metapelites from the Algyő–Ferencszállás area, SE Hungary: thermobarometric constraints from coexisting mineral assemblages and garnet zoning. Acta Geol Hung 45:1–27

Horváth P, Balen D, Finger F, Tomljenović B, Krenn E (2010) Contrasting P-T-t paths from the basement of the Tisia Unit (Slavonian Mts., NE Croatia): application of quantitative phase diagrams and monazite age dating. Lithos 117:269–282

Hoschek G (1967) Untersuchungen zum Stabilitätsbereich von Chloritoid und Staurolith. Contrib Mineral Petrol 14:123–162

Hoschek G (1969) The stability of staurolite and chloritoid and their significance in metamorphism of pelitic rocks. Contrib Mineral Petrol 22:208–232

Jamičić D (1983) Strukturni sklop metamorfnih stijena Krndije i južnih padina Papuka (Structural fabric of the metamorphosed rocks of Mt. Krndija and the eastern part of Mt.Papuk). Geol vjesnik Zagreb 36:51–72 (in Croatian)

Jamičić D (1988) Strukturni sklop slavonskih planina (Tectonics of the Slavonian Mts.). PhD thesis, University of Zagreb, pp 152 (in Croatian)

Jamičić D (1989) Basic geological map of Yugoslavia in scale 1:100.000, sheet Daruvar. Geol Inst Zagreb, Fed Geol Inst Beograd

Jamičić D, Brkić M (1987) Basic geological map of Yugoslavia in scale 1:100.000, sheet Orahovica. Geol Inst Zagreb, Fed Geol Inst Beograd

Jamičić D, Brkić M, Crnko J, Vragović M (1986) Basic geological map of Yugoslavia–explanatory notes for sheet Orahovica. Geol Inst Zagreb, Fed Geol Inst Beograd

Janots E, Engi M, Berger A, Allaz J, Schwarz JO, Spandler C (2008) Prograde metamorphic sequence of REE minerals in pelitic rocks of the Central Alps: implications for allanite-monazite-xenotime phase relations from 250 to 610 degrees C. J Metamorph Geol 26:509–526

Koroknai B, Horváth P, Németh T, Pelikán P (2000) Chloritoid schists from the Uppony and Szendrö Paleozoic (NE Hungary): implications for Alpine structural and metamorphic evolution. Slovak Geol Mag 6:269–272

Koroknai B, Horváth P, Németh T (2001) Chloritoid schists from the Uppony Mts (NE Hungary): mineralogical, petrological and structural data from a new occurrence. Acta Geol Hung 44: 47–65

Kositcin N, McNaughton NJ, Neal J, Griffen BJ, Fletcher IR, Groves DI, Rasmussen B (2003) Textural and geochemical discrimination between xenotime of different origin in the Archean Witwatersrand basin, South Africa. Geochim Cosmochim Acta 67:709–731

Krenn E, Ustaszewski K, Finger F (2008) Detrital and newly formed metamorphic monazite in amphibolite-facies metapelites from the Motajica Massif, Bosnia. Chem Geol 254:164–174

Lelkes-Felvári G, Árkai P, Sassi FP, Balogh K (1996) Main features of the regional metamorphic events in Hungary: a review. Geol Carpathica 47:257–270

Lelkes-Felvári G, Frank W, Schuster R (2003) Geochronological constraints of the Variscan, Permian-Triassic and eo-Alpine (Cretaceous) evolution of the Great Hungarian Plain basement. Geol Carpathica 54:299–315

Márton E (2000) The Tisza megatectonic unit in the light of paleomagnetic data. Acta Geol Hung 43:329–343

Massonne HJ, Schreyer W (1987) Phengite geobarometry based on the limiting assemblage with K-feldspar, phlogopite, and quartz. Contrib Mineral Petrol 96:212–224

McLennan SM (2001) Relationships between the trace element composition of sedimentary rocks and upper continental crust. Geochem Geophys Geosyst 2:1021. doi:10.1029/2000GC000109

McLennan SM, Taylor SR (1991) Sedimentary rocks and crustal evolution: tectonic setting and secular trends. J Geol 99:1–21

Messiga B, Kienast JR, Rebay G, Riccardi P, Tribuzio R (1999) Cr-rich magnesiochloritoid eclogites from the Monviso ophiolites (Western Alps, Italy). J Metamorph Geol 17:287–299

Montel JM, Foret S, Veschambre M, Nicollet Ch, Provost A (1996) Electron microprobe dating of monazite. Chem Geol 131:37–53

Overstreet WC (1967) The geologic occurrence of monazite. US Geological Survey Professional Paper 530

Pamić J, Jamičić D (1986) Metabasic intrusive rocks from the Paleozoic Radlovac complex of Mt. Papuk in Slavonija (northern Croatia). Rad Jugosl Akad Znan Umjet Zagreb 424:97–125

Pamić J, Jurković I (2002) Paleozoic tectonostratigraphic units in the northwest and central Dinarides and the adjoining South Tisia. Int J Earth Sci 91:538–554

Pamić J, Lanphere M (1991) Hercynian granites and metamorphic rocks from the Papuk, Psunj, Krndija and the surrounding basement of the Pannonian Basin (Northern Croatia, Yugoslavia). Geologija Ljubljana 34:81–253

Pamić J, Lanphere M, McKee E (1988) Radiometric ages of metamorphic and associated igneous rocks of the Slavonian Mountains in the southern part of the Pannonian Basin, Yugoslavia. Acta Geol Zagreb 18:13–39

Pamić J, Balen D, Tibljaš D (2002) Petrology and geochemistry of orthoamphibolites from the Variscan metamorphic sequences of the South Tisia in Croatia—an overview with geodynamic implications. Int J Earth Sci 91:787–798

Pouchou JL, Pichoir F (1984) A new model for quantitative X-ray microanalyses, Part I. Application to the analyses of homogenous samples. La Recherche Aerospatiale 3:13–38

Powell R, Holland TJB, Worley B (1998) Calculating phase diagrams involving solid solutions via non-linear equations, with examples using THERMOCALC. J Metamorph Geol 16:577–588

Pyle J, Spear F, Wark DA (2002) Electron microprobe analysis of REE in apatite, monazite and xenotime: protocols and pitfalls. In: Kohn ML, Rakovan J, Hughes JM (eds) Phosphates: geochemical, geobiological and materials importance. Reviews in Mineralogy and Geochemistry 48:337–362

Rasmussen B, Muhling JR (2007) Monazite begets monazite: evidence for dissolution of detrital monazite and reprecipitation of syntectonic monazite during low-grade regional metamorphism. Contrib Mineral Petrol 154:675–689

Rasmussen B, Fletcher IR, Muhling JR, Wilde SA (2010) In situ U-Th-Pb geochronology of monazite and xenotime from the Jack Hills belt: implications for the age of deposition and metamorphism of Hadean zircons. Precambr Res 180:26–46

Rosenberg PE (2002) The nature, formation, and stability of end-member illite: a hypothesis. Am Min 87:103–107

Schmid SM, Bernoulli D, Fügenschuh B, Matenco L, Schefer S, Schuster R, Tischler M, Ustaszewski K (2008) The Alps–Carpathians–Dinarides connection: a compilation of tectonic units. Swiss J Geosci 101:139–183

Simon G, Chopin C, Schenk V (1997) Near-end-member magnesiochloritoid in prograde-zoned pyrope, Dora-Maira massif, western Alps. Lithos 41:37–57

Slovenec D (1986) Nalazi pirofilita, paragonita, margarita i glaukonita u stijenama slavonskih planina (Registrations of Pyrophyllite,

Paragonite, Margarite and Glauconite in the Rocks of the Slavonian Mountains). Geol vjesnik Zagreb 39:61–74 (in Croatian)

Spear FS (1993) Metamorphic phase equilibria and pressure-temperature-time paths. Mineral Soc Am Monograph, Washington

Suzuki K, Adachi M (1991) Precambrian provenance and Silurian metamorphism of the Tsubonasawa paragneiss in the South Kitakami terrane, Northwest Japan, revealed by the chemical Th-U-total Pb isochron ages of monazite, zircon and xenotime. Geochem J 25:357–376

Suzuki K, Adachi M, Tanaka T (1991) Middle Precambrian provenance of Jurassic sandstone in the Mino Terrane, central Japan: Th-U-total Pb evidence from an electron microprobe monazite study. Sedimentary Geol 75:141–147

Taylor SR, McLennan SM (1985) The continental crust: its composition and evolution. Blackwell, Oxford

Ustaszewski K, Kounov A, Schmid SM, Schaltegger U, Krenn E, Frank W, Fügenschuh B (2010) Evolution of the Adria-Europe plate boundary in the northern Dinarides: from continent–continent collision to back-arc extension. Tectonics 29:TC6017. doi:10.1029/2010TC002668

Vallini D, Rasmussen B, Krapež B, Fletcher IR, McNaughton N (2005) Microtextures, geochemistry and geochronology of authigenic xenotime: constraining the cementation history of a Palaeoproterozoic metasedimentary sequence. Sedimentology 52:101–122

Varga AR, Szakmány G (2004) Geochemistry and provenance of the upper carboniferous sandstones from borehole Diósviszló-3 (Téseny Sandstone Formation, SW Hungary). Acta Mineral Petrogr Szeged 45:7–14

Varga A, Szakmány Gy, Árgyelán T, Józsa S, Raucsik B, Máthé Z (2007) Complex examination of the upper paleozoic siliciclastic rocks from southern Transdanubia, SW Hungary—mineralogical, petrographic, and geochemical study. In: Arribas J, Critelli S, Johnsson MJ (eds) Sedimentary provenance and petrogenesis: perspectives from petrography and geochemistry. Geol Soc Am Spec Paper 420:221–240

Velić I, Vlahović I (eds) (2009) Tumač Geološke karte Republike Hrvatske 1:300.000 (Explanatory notes for geological map of Croatia 1.300.000). Hrvatski geološki institut Zagreb

Vidal O, Parra T (2000) Exhumation paths of high-pressure metapelites obtained from local equilibria for chlorite-phengite assemblages. Geol J 35:139–161

Vidal O, Theye T, Chopin C (1994) Experimental study of chloritoid stability at high pressure and various fO_2 conditions. Contrib Mineral Petrol 118:256–270

Vidal O, Goffé B, Bousquet R, Parra T (1999) Calibration and testing of an empirical chloritoid-chlorite Mg-Fe exchange thermometer and thermodynamic data for daphnite. J Metamorph Geol 17: 25–39

Vragović M, Majer V (1979a) Kloritoidni škriljci u metamorfnim kompleksima u sjevernoj Hrvatskoj (Jugoslavija) (Chloritoid schists in the metamorphic complexes in northern Croatia (Yugoslavia)). Geol vjesnik Zagreb 31:287–294 (in Croatian)

Vragović M, Majer V (1979b) Prilozi za poznavanje metamorfnih stijena Zagrebačke gore, Moslavačke gore i Papuka (Hrvatska, Jugoslavija) (Metamorphosed ultramafic rocks from Papuk Mountain, cordierite rocks from Moslavačka mountain, and chloritoid-bearing metapelites from Zagrebačka mountain, northern Yugoslavia). Geol vjesnik Zagreb 31:295–308 (in Croatian)